Experimental Study on the Strength and Deformation Characteristics of Shield Wall for BWR Type Reactor Building

M. Watabe
University of Tokyo Metropolitan, Architectural Dept., 2-1-1, Fukazawa, Setagaya-ku, Tokyo 158, Japan
T. Kubo
Nagoya Institute of Technology, Structural Engineering Dept., Gokisho-machi, Showa-ku, Nagoya 466, Japan
N. Machida, T. Shibuya, Y. Tamamura, I. Shiraishi, I. Kurihara, Y. Nakamura
Kumagai-Gumi Co., Ltd., Nuclear Development Div., 17-1 Tsukudo-cho, Shinjuku-ku, Tokyo 162, Japan
O. Tanaka, T. Masao, A. Mikame, T. Fukushi, K. Uchida
Fujita Technical Research Division, 74, Otana-cho, Kohoku-ku, Yokohama 223, Japan

ABSTRACT

In this paper, described are elasto-plastic behaviors of circular truncated conical and cylindrical shear walls subjected to a severe seismic lateral loading. The major purpose of this study is to reveal load-deformation characteristics of the shear walls with emphasis upon strength and deformation. Correlation study of theoretical analyses with experimental results is also made through various approaches such as conventional empirical formulae, an elastic theory and a non-linear FEM analysis. Verification of employing experimental methods utilizing half-symmetrical model is refferred to as well.

1. Introduction

For the purpose of obtaining more realistic strength and deformation characteristics of a BWR type reactor building, of which schematic elevation is shown in Fig. 1, excited by severe earthquake ground motions, the following experimental and correlating analytical studies have been carried out. The experimental study is indispensable for the above purpose, due to the fact that a BWR type reactor building is especially complicated with its structural elements such as outer and inner walls and a shielding wall. Among these walls, inner and shielding walls constitute main structural elements to resist lateral forces during an earthquake as "shear walls". In order to evaluate the safety margin at the ultimate state of these shear walls due to lateral earthquake forces, experimental back-up data have been required. Experimental exploration is demonstrated to verify the employment of a half-symmetrical model instead of a full-shaped model. This half-symmetrical model might expose a clear view of crack pattern during the experiment, and reduce the required lateral loading capacities for the experiment.

The main objectives of this study can be summarized as follows: (1) acquisition of extensive knowledge on the strength and deformation characteristics of a shield wall subjected to lateral forces; (2) investigation on the expected discrepancies between the results obtained from a full-shaped specimen and those from a half-symmetrical specimen.

2. Specimens

Specification of the specimens and properties of the materials are shown in Table I. Figures 2 (a) and (b) show the shapes of circular truncated conical and cylindrical shear walls, respectively. The specimens are about 1/25 scaled in their dimensions. For each shear

wall, both a full-shaped model and a half-symmetrical model have been prepared.Shear walls are 80 mm in thickness and are arranged in both longitudinal and transverse directions with double D6-reinforcing bars of SD35 (JIS Standard). The maximum diameter of concrete aggregates is 10mm, and the design compressive strength of concrete is taken to 240 kg/cm^2.

3. Loading Procedures

Among the experiments, lateral forces have been reversely applied to the loading slab of a specimen under displacement control in accordance with the loading schedule indicated in Fig. 3 simulating the behavior of a reactor building during an earthquake. Axial forces have been applied to be 20 kg/cm^2 at the bottom of shear wall. At experiments on the half-symmetrical models, devices shown in Fig. 4 were placed at the ends of the loading slab to restrict the specimens from excessive torsion and sway.

4. Elasto-plastic Analysis by a Finite Element Method

In the FEM anlysis, the circular truncated conical shear wall shown in Fig. 5 has been represented by a set of planner shell elements with 4 nodal points. Non-linear properties of elements along the thickness of the wall are described by use of the composite layered elements consisting of both concrete and steel layers. For the constitutive law of concrete, that proposed by Darwin and Pecknold is adopted, while the compressive strength in the direction parallel to crack is decreased in accordance with the Collins' experimental results (1). Effects of the aggregate interlock between cracks are taken into account by use of formula proposed by Aoyagi (2). Effects of the bond between reinforcing bar and concrete are expressed by Shirai's approach (3) . The stress-strain relation for the reinforcing bar is given by a perfect elasto-plastic model. Figure 6 shows the resultant features of the stress-strain relation of concrete.

5. Experimental Results and Analytical Results

5.1 Circular Truncated Conical Shear Wall

The results obtained from the experiment such as the initial stiffness, the cracking loads, and the ultimate strength with its failure mode are tabulated in Table II. The crack pattern at the final state and the load-deformation curves are given in Figs. 7 and 8, respectively. In tabel II, the results obtained from the FEM analysis and those obtained by the elastic beam theory and conventional empirical formulae are included. The comparison between experimental and analytical results has been made.

The elastic beam theory and conventional empirical formulae employed in this study are shown in eqs. (1) to (4).

Initial stiffness by elastic beam theory

$$K_I = 1 \Big/ \left(\int \frac{x^2}{Ec \cdot Ie(x)}\, dx + K \int \frac{1}{Gc \cdot Aw(x)}\, dx \right) \quad \cdots\cdots \quad \text{eq. - (1)}$$

Flexural cracking load

$$Q_{FC} = (Ft + \sigma o) \cdot Ze \Big/ h \quad \cdots\cdots \quad \text{eq. - (2)}$$

Shear cracking load proposed by Ohno (4)

$$Q_{SC} = \frac{0.0612(500 + Fc)}{M/QD + 1.7} \cdot \left(1 + \frac{\sigma o}{150}\right) \cdot Aw \text{ bottom} \quad \cdots\cdots \quad \text{eq. - (3)}$$

Ultimate load

$$Q_{SU} = (Pw \cdot s\sigma y + \sigma o)\ ave. \cdot Aw_{top} \qquad \ldots\ldots \quad eq. - (4)$$

χ : Shape factor

Ie, Ze : Geometrical moment of inertia and section modulus, respectively.

Aw bottom, Aw top : Half of the section area at the bottom and the top of specimen, respectively.

Other notations in eqs. (1) to (4) are found in Table I.

5.1.1 Failure Mode The failure modes of both a full-shaped and a half-symmetrical specimens are as follows : 1) The initial flexural crack has been observed at the lowest part of the tensile flange at the rotation angle R = 0.3 to 0.4 x 10^{-3} rad. 2) With the rotation angle R = 0.5 to 0.6 x 10^{-3}rad., the initial shear crack has been found at the upper part of the web portion of the wall. 3) When R = 1.0 to 2.0 x 10^{-3} rad., these cracks have progressed. 4) With the rotation angle of R = 4.0 x 10^{-3} rad., the exfoliation and crushing of concrete have occurred at the upper part of the wall.

The maximum lateral load of the full-shaped specimen is obtained at the rotation angle R = 6.0 x 10^{-3} rad. during the first loading cycle. The corresponding failure mode is the shear slippage at the top of web portion of the wall. The maximum load of the half-symmetrical specimen, similarly, is obtained at R = 6.0 x 10^{-3} rad. within the first loading cycle. The peak loads obtained at R = 6.0 x 10^{-3} rad. are gradually decreased as the number of cycles increases, and the identical failure mode to that of the full-shaped specimen, i.e. the shear slippage, occurs at the rotation angle R = 7.2 x 10^{-3} rad.

5.1.2 Load-Deformation Characteristics Load-deformation curves of these two specimens are well represented by the origin-oriented hysteresis rule with the rotation angle R smaller than 2.0 x 10^{-3} rad., by the rule connecting bewteen points of maximum and minimum in the previous state within the R of 2.0 x 10^{-3} rad. and 4.0 x 10^{-3} rad., and by the inverted S shaped hysteresis rule with R larger than 4.0 x 10^{-3} rad.

5.1.3 Flexural and Shear Deformation Components The relation between the rotation angle of the specimens and the deformation is summarized in Table III. The total deformation of the specimen is decomposed into flexural and shear deformation. The ratios of the flexural deformation to the total deformation, and those of the shear deformation are tabulated in Table III. The flexural deformation is estimated by integration of curvatures along height of the wall, and the shear deformation is determined by subtracting the flexural deformation from the total deformation of the specimen at the corresponding state. The comparison of the results obtained from the two specimens leads to the finding that the ratios of the flexural deformation to the total deformation of the half-symmetrical specimen are slightly larger than those of the full-shaped specimen.

5.2 Cylindrical Shear Wall

Experimental results obtained during the loading are summarized in Table II, and Figs. 9, 10 and 11. The initial stiffness, the cracking and yielding loads and the ultimate strength and so on are listed in Table II. Final pattern of cracks generated during the experiment is shown in Fig. 9, load-deformation curves for specimens of a full-shaped model and that of a half symmetrical model are described in Figs. 10 (a) and (b), respectively. Figure 11 shows the envelope curves for relations between shear stresses determined for the cross area and rotation angles of the specimen.

5.2.1 Failure Mode For both a full-shaped and a half-symmetrical specimens, the failure

modes are as follows: 1) Flexural cracks have occurred at the bottom of the tensile flange portion of the wall. 2) Diagonal shear cracks have been observed at the center of web portion of the wall. These cracks have occurred simultaneously on the both outer and inner sides of the wall. 3) Tensile reinforcing bars in the longitudinal direction, i.e. along the height of the wall, have been yielded at the bottom of the flange portion. Consequently yielding zone has been extended from the bottom to the mid-point of the wall. 4) Reinforcing bars in the transverse direction, i.e. along the circumference of the cylindrical wall, have been yielded. 5) Crush of concrete caused by shear compression then has been produced at the bottom of the wall in the web portion with the some extention when the rotation angle R equals to 10 - 16 x 10^{-3} rad. 6) Final failure modes of the specimens have been shear compression failures, and they have caused to deteriorate the strength. No significant difference in both specimens has been observed in their either crack pattern or number and width of cracks.

5.2.2 Load-Deformation Characteristics The initial stiffness of the half-symmetrical cylindrical wall is 0.49 times that of the full-shaped cylindrical wall. The expected ratio of the initial stiffness for the these two is 0.5. From a set of Figs.10 and 11, it can be found that the strength of the half-symmetrical wall is slightly larger than that of the full-shaped wall within the deformation of the rotation angle R being less than 8 x 10^{-3} rad. No significant difference, however, has been recognized in the characteristics of hysteresis rules. Hysteresis rules for these two specimens are almost identical with each other.

The half-symmetrical specimen possesses both the greater ductility capacity and the larger strength than the full-shaped specimen, while the former specimen reveals an almost identical failure mode to the latter specimen.

5.2.3 Distribution of Shear Stresses of Concrete at the Elastic State Distributions of shear stresses of concrete taken across the mid-point of the walls are shown in Fig. 12. The values of shear stresses are normalized by the average value determined by the total lateral load divided by the total cross sectional area. The distribution of stresses along the inner circumferencial side is larger than along the outer circumferencial side. Based upon the elastic beam theory, the shape factor of shear of a cylinder shaped section is 2.0. The empirical shape factors as described in Fig. 12 for both full-shaped and half-symmetrical walls are nearly 1.5 along the outer circumferencila side. The empirical factor obtained during the test is smaller than the theoretical one. The factors obtained at the inner circumferencial side are almost 2.0 for the specimens, and coincide with the factors from the theoretical analysis. Comparison between shape factors obtained from the full-shaped and half-symmetrical specimens leads to the finding that along the inner circumferencial side they have slight discrepancy with each other, while along the outer circumferencial side they coincide well with each other.

5.2.4 Behavior of Reinforcing Bars The envelope of stress-strain relations of reinfocing bars is shown in Fig. 13. Figures 13 (a) and (b) represent the results for bars along longitudinal direction and those along transverse direction, respectively. The strains of the reinforcing bars placed in the outer side of the walls are generally larger than those in the inner side. This tendency is found either for the bars in longitudinal direction or for those in transverse direction for both the two types of specimens. No significant difference is recognized on the shapes of stress-strain relationship of full-shaped and

half-symmetrical specimens.

6. Concluding Statements

Following conclusive remarks are obtained through empirical and analytical studies.

(1) A realistic load-deformation characteristics of circular truncated conical and cylindrical shear walls has been established. Failure processes of these shear walls also have been obtained. Detailed behaviors of reinforcing bars and concrete such as stress-strain relationship are described during the experiments.

(2) The comparison of the test results obtained from full-shaped and half-symmetrical specimens leads to the fact that the use of a half-symmetrical model is proper and effective in place of a full-shaped model.

(3) Strength causing cracks in concrete, that causing yield of tensile reinforcing bar, and the ultimate strength of shear walls determined by the F.E.M. analysis and conventional empirical formulae correspond well to those experimental values obtained by loading tests. By use of the F.E.M. analysis, one can estimate the load-deformation characteristics within the small deformation, i.e. within the range of rotation angle R less than 4.0×10^{-3} rad.

7. Acknowledgment

These studies have been carried out as part of a joint research by the "Study Committee on Load-Deflection Characteristics of Nuclear Reactor Building Structures" of the Kenchiku Kenkyu Shinko Kyokai.

8. References

/1/ Collins M. P. et al. : "THE RESPONSE OF REINFORCED CONCRETE TO IN-PLANE SHEAR AND NORMAL STRESSES", Univ. of Tronto, Department of Civil Engineering, March 1982.

/2/ Aoyagi M. : "In-Plane Shear in Reinforced Concrete Shell Elements", PROCEEDINGS OF JCI COLLOQUIUM ON SHEAR ANALYSIS OF RC STRUCTURES, June 1982.

/3/ Shirai N. et al. : "Hysteretic Characteristics of Reinforced Concrete Shear Wall and Inelstic Analysis", Summaries of Technical Papers of Annual Meeting, Architectural Institute of Japan, 1980.

/4/ Ohno K. et al. : "Study on Shear Strength Formula of Reinforced Concrete Columns", Study Report of Hokkaido Office of Architectural Institute of Japan, March 1978.

Table I Properties of specimens

Properties \ Test Specimens				Circular Truncated Conical Shear Wall		Cylindrical Shear Wall	
	Shape Model			Full-Shaped	Half-Symmetrical	Full-Shaped	Half-Symmetrical
Dimensions of Test Specimens	Wall Thickness(mm)		tw	80		80	
	Shear Span Ratio		M/QD	0.8		1.0	
	Reinforcement Ratio(%)	Vertical	Pwv	1.5(at the Base) 2.5(at the Top)		1.6	
		Horizontal	Pwh	1.5		1.6	
	Axial Stress (kg/cm²)		σo	20		0	
Material properties of Concrete	Compressive Strength (kg/cm²)		Fc	272	248	281	294
	Young's Modulus (kg/cm²)		Ec	2.30×10^5	2.20×10^5	1.53×10^5	1.67×10^5
	Poisson's Ratio		ν	0.16	0.16	0.15	0.17
	Cleavage Strength (kg/cm²)		Ft	19.4	20.7	24.1	14.1
Material Properties of Re.Bars	Yield Strength (kg/cm²)		sσy	4072		4017	
	Young's Modulus (kg/cm²)		Es	1.77×10^6		1.80×10^6	

Table II Experimental results of circular truncated conical and cylindrical shear walls.

Test Specimens / Experimental Results		Circular Truncated Conical Shear Wall				Clyndrical Shear Wall			
		Test	Test / Cal.	Test / FEM Ana.	Test of Half / Test of Full	Test	Test / Cal.	Test / FEM Ana.	Test of Half / Test of Full
Initial Stiffness (ton/cm)	Full	926	0.85	0.76	0.55	653	0.98	1.24	0.49
	Half	506	0.96	0.96		320	0.89	1.18	
Flexural Cracking Load(ton)	Full	31.2	0.88	1.04	0.51	19.7	0.53	0.97	0.48
	Half	16.0	0.90	1.07		9.5	0.54	0.94	
Shear Cracking Load(ton)	Full	41.5	1.28	1.04	0.43	32.0	0.90	0.90	0.47
	Half	17.6	1.12	1.17		15.1	0.83	0.86	
Yielding Load of Verti. Reinforcing Bar at Web Zone(ton)	Full	90.2	—	1.02	0.48	91.7	1.12	0.89	0.53
	Half	43.2	—	1.02		48.8	1.18	0.91	
Yielding Load of Horiz. Reinforcing Bar at Web Zone(ton)	Full	90.2	—	0.93	0.44	88.8	—	0.73	0.60
	Half	39.0	—	0.82		52.9	—	0.86	
Ultimate Shear Strength(ton)	Full	97.5	1.07	0.85	0.49	105.2	0.81	—	0.54
	Half	47.3	1.04	1.00		56.9	0.87	—	
Failure Mode	Full	Shear-Slip Failure				Shear-Compressive Failure			
	Half	Shear-Slip Failure				Shear-Compressive Failare			

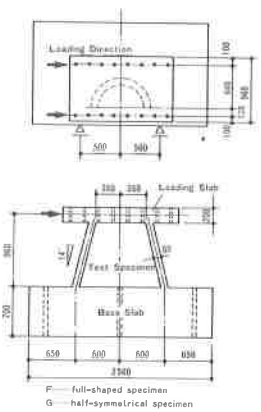

(a) Circular truncated conical shear wall

Table III Ratio of flexural and shear deformations to the total deformation of the circular truncated shear wall. (unit %)

Test Specimens \ Rotation Angle of Member	1/4000	1/2000	1/1000	2/1000	4/1000	6/1000
Full-Shaped Model	50 / 50	51 / 49	45 / 55	43 / 57	35 / 65	35 / 65
Half Symmetrical Model	42 / 58	43 / 57	40 / 60	37 / 63	37 / 63	33 / 67

The upper and lower figures indicate flexural and shear deformations to the total deformation, respectively.

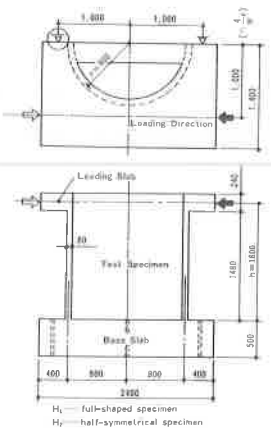

(b) cylindrical shear wall

Fig. 2 Half-symmetrical model of specimen

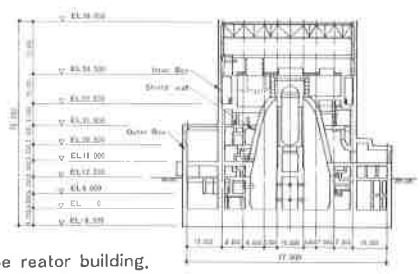
Fig. 1 BWR type reator building.

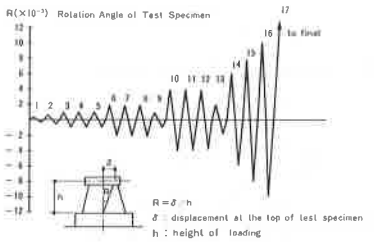

Fig. 3 Loading schedule.

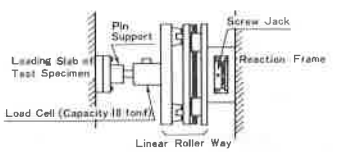

Fig. 4 Details of the device for restrictions of torsional and sway motions.

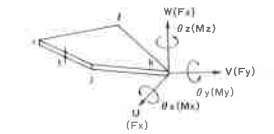

(a) isoparametric Planmar shell element with 4 nodal Points

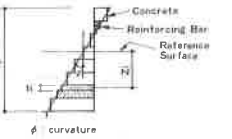

(b) laminated element and strain distribution

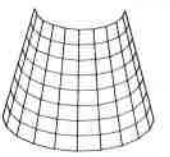

(c) model of a circular truncated conical shear wall

Fig. 5 Model for F.E.M.

A－B : $E=(0.5f_t+\sigma_a)/\varepsilon_a$
B－C : $E=(0.5f_t+\sigma_t)/\varepsilon_t$
C－D : $E=(0.5f_t+\sigma_a)/\varepsilon_a$
D－A : $E=(\sigma_a-\sigma_t)/(\varepsilon_a-\varepsilon_t)$
0－A : $E=\sigma_a/\varepsilon_a$
$\varepsilon_{bu}=_s\varepsilon_{y_1}$ $\alpha=0.3$

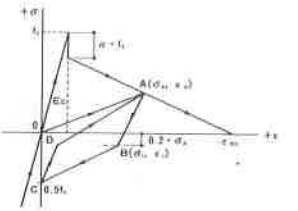

Fig. 6 Stress-strain relation of concrete.

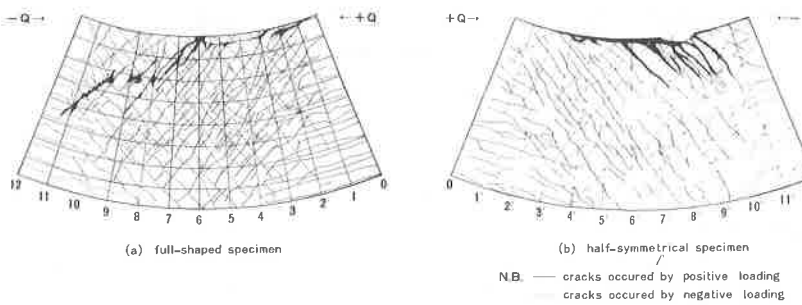

Fig. 7 Crack patterns at the final state of the circular truncated conical shear wall.

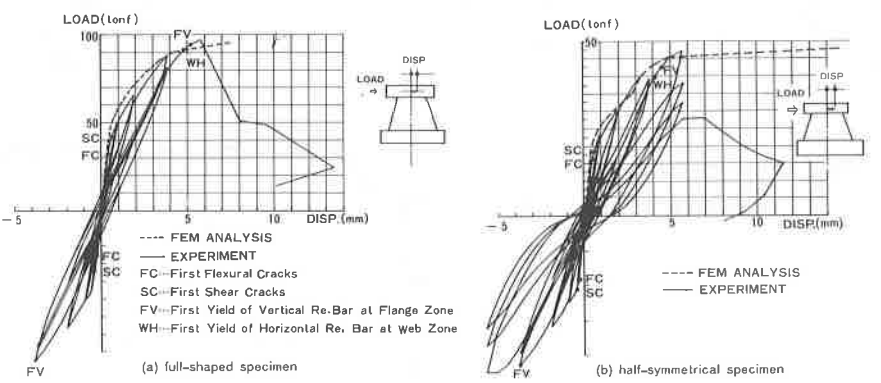

Fig. 8 Load-deformation curve of the circular truncated conical shear wall.

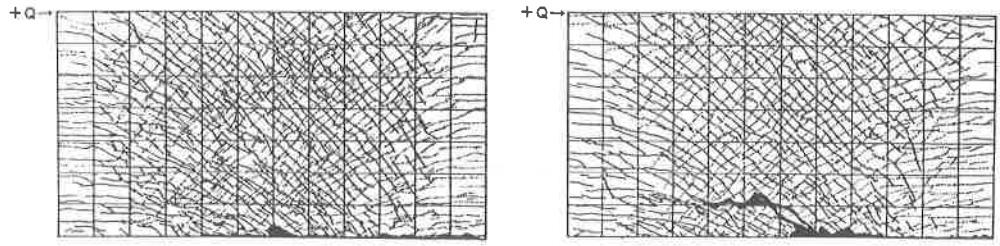

(a) full-shaped specimen (b) half-symmetrical specimen

Fig. 9 Crack patterns at the final state of the cylindrical shear wall.

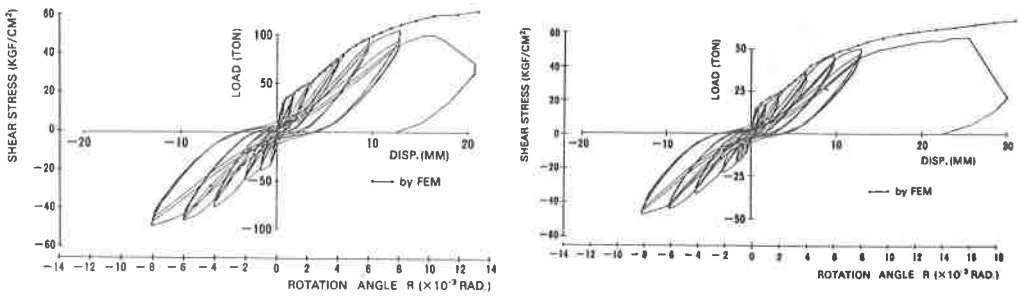

(a) full-shaped specimen (b) half-symmetrical specimen

Fig. 10 Load-deformation curve of the cylindrical shear wall.

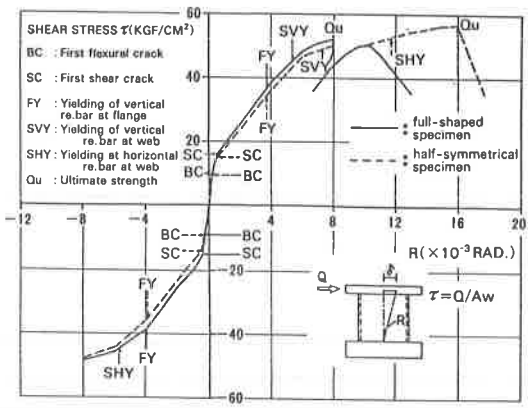

Fig. 11 Envelope curve of the shear stress-rotation angle.

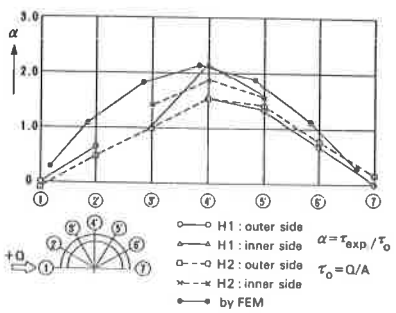

Fig.12 Distribution of shear stress at the elastic state.

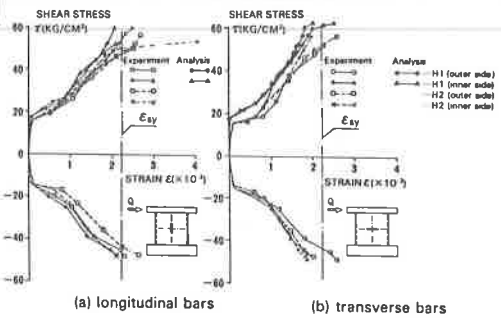

(a) longitudinal bars (b) transverse bars

Fig.13 Shear stress-strain curves of the reinforcement at the web portion.